

Improvement of crystal quality and optical property in (11-22) semipolar InGaN/GaN light emitting diodes grown on hemi-spherically patterned SiO₂ mask

Daehong Min^a, Geunho Yoo^a, Yongwoo Ryu^a, Seunghwan Moon^a, Kyuho Lee^b and Okhyun Nam^{a,*}

^aLED Technology Center, Department of Nano-Optical Engineering, Korea Polytechnic University, Siheung 429-793, Korea

^bR&D Center, Seoul Optodevice., Ltd, Ansan 425-851, Korea

We report the improved crystal quality and optical property in (11-22) semipolar InGaN/GaN light emitting diodes (LEDs) grown on hemi-spherically patterned SiO₂ mask on m-plane sapphire substrate (HP-SiO₂) compared with the m-plane sapphire substrate (m-planar), using metalorganic chemical vapor deposition (MOCVD). The photoluminescence (PL) results showed that the integrated intensity of the near band edge (NBE) emission of the GaN layer grown on HP-SiO₂ was increased by 3 times as high as that of m-planar. The full width at half maximums (FWHMs) of X-ray rocking curves for the on- and off-axis planes of the GaN layers on HP-SiO₂ were narrower down than on m-planar, which indicates that the crystal quality of the semipolar GaN layers on HP-SiO₂ was considerably improved as compared with that on m-planar by reducing defects such as perfect/partial dislocations and basal stacking faults. Cross-sectional transmission electron microscopy (TEM) images also showed the reduction of dislocation density in GaN layers on HP-SiO₂ than on m-planar. The optical power of InGaN/GaN LEDs with HP-SiO₂ was increased by 1.7 and 7.3 times at injection current of 20 mA and 100 mA, respectively, in comparison with the m-planar LEDs.

Key words: Semipolar GaN, Hemispherically SiO₂ mask, Patterned sapphire substrate, Lateral over growth, Metalorganic chemical vapor deposition.

Introduction

In general, c-plane InGaN/GaN multi-quantum-well structure is widely used in blue and green light emitting diodes (LEDs) [1-2]. However, in the c-plane polar structure of InGaN/GaN quantum wells (QWs), strong spontaneous and piezoelectric polarizations exist [3]. These polarizations lead to large electric fields separating electron and hole wave functions [4]. Therefore, the radiative recombination lifetime in the films increases, which raises the probability of non-radiative recombination and decreases the achievable internal quantum efficiency in InGaN/GaN quantum wells [5-6]. To solve these problems, many research groups have studied non-polar [7-8] and semipolar GaN and InGaN/GaN LEDs [9-10], which could reduce polarization-induced electrostatic fields. Especially, the specific features of (11-22) semipolar InGaN/GaN structures are emphasized, which can be beneficial for improving the optical and transport properties of quantum-well based light emitting devices in comparison with those of non-polar structures [11]. However, semipolar hetero-epitaxial structures grown in (11-22) crystal orientation suffer from a high density of defects such as basal stacking faults (BSFs), several types of perfect dislocations, and partial dislocations

(PDs) terminating the BSFs [12]. To reduce these defects, several research groups have reported on the use of SiO₂ mask and patterned sapphire [13-17]. Actually, for improved performance of the LEDs, we need to achieve high extraction efficiency as well as the low defect density in epi structure of LEDs. In general, the use of a hemispherical patterned sapphire substrate is known to be beneficial to improve light extraction efficiency [18]. Therefore, in this study, we report an improvement of the crystal quality and optical property of the (11-22) semipolar InGaN/GaN LEDs grown on hemispherically patterned SiO₂ mask.

Experimental

Figs. 1(a)-(d) show a schematic of the substrate preparation process to prepare the HP-SiO₂ mask on sapphire substrate. As shown in Fig. 1(a), firstly, 1.1 μm SiO₂ layers were deposited on the m-plane sapphire substrates by plasma-enhanced chemical vapor deposition (PECVD). Secondly, a positive photoresist (PR) was coated and patterned with 2 × 2 μm² using a mask aligner with a deep ultraviolet lamp, as shown in Fig. 1(b). Then they were shaped into hemispherical PR patterns using a thermal reflow technique and HP-SiO₂ mask was formed by inductively coupled plasma (ICP) etching with C₄F₈ based plasmas, respectively, as shown in Figs. 1(c)-(d). For (11-22) semipolar GaN template layer growth, two step growth methods were used for improving the surface morphology and crystal

*Corresponding author:
Tel : +82-31-8041-0718
Fax: +82-31-8041-1917
E-mail: ohnam@kpu.ac.kr

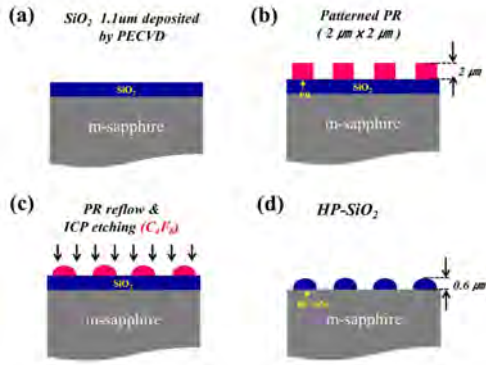


Fig. 1. Schematic of the substrate preparation process.

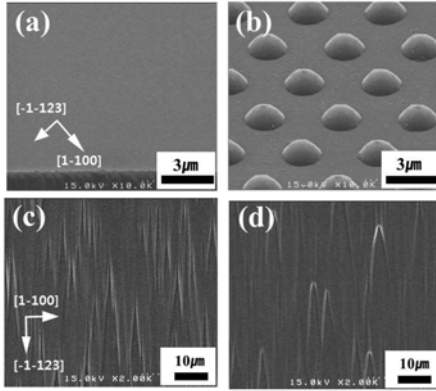


Fig. 2. SEM images of (a) m-planar and (b) HP-SiO₂ substrates, respectively. The surface morphology of the (11-22) GaN layers with the thickness of 6 μm grown on (c) m-planar and (d) HP-SiO₂, respectively.

quality of GaN layers on m-planar and HP-SiO₂ substrates using metalorganic chemical vapor deposition (MOCVD) [19]. The surface morphology of the semipolar GaN layer was observed by scanning electron microscopy (SEM). The room-temperature (RT) and low-temperature (LT) photoluminescence (PL) analyses were conducted using the 325 nm line of a He-Cd laser to investigate the luminescence characteristics at 300 K and 18 K, respectively. The crystal quality of the GaN layers was measured using a omega scan of double crystal X-ray diffraction (DCXRD). The cross-section microstructure of the GaN layer was observed by transmission electron microscopy (TEM). The optical power of (11-22) semipolar InGaN/GaN LEDs was measured by electroluminescence (EL) measurement on the tops of processed LED chips fabricated with a size of 400 × 400 μm².

Results and Discussion

Figs. 2(a)-(b) show the SEM images of m-planar and HP-SiO₂ substrates, respectively. HP-SiO₂ patterns were formed with a diameter of 2 μm, a height of 0.6 μm, and as interval for 2 μm for each pattern. Figs. 2(c)-(d) show the SEM images of surface morphology of the (11-22) GaN layers with the thickness of 6 μm grown on m-planar and HP-SiO₂, respectively. All samples

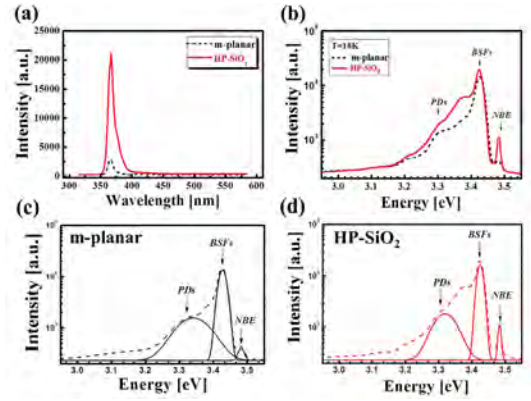


Fig. 3. (a) Room temperature PL spectra and (b) low temperature PL spectra of the (11-22) GaN layers on m-planar and HP-SiO₂. The low temperature spectra were resolved into individual peaks [(c) and (d)] by using a multi-Gaussian fitting (solid line). The peaks related with PDs, BSFs and NBE were found to be at 3.32 eV, 3.42 eV, and 3.48 eV, respectively.

Table 1. The LT-PL integrated intensity ratio of the BSFs and PDs to the NBE.

	I_{BSFs}/I_{NBE}	I_{PDs}/I_{NBE}
m-planar	81	38
HP-SiO ₂	38	14

show arrowhead-like feature along the [-1-123] direction which is caused by the anisotropic diffusion length of surface adatoms toward crystallographic directions such as [11-2-3] and [1-100] owing to the crystallographic difference between m-plane sapphire and (11-22) semipolar GaN [20]. Also, the arrow-head shape of (11-22) semipolar GaN surface on HP-SiO₂ is wider than that of m-planar, which is attributed to the relaxation of anisotropic growth by enhanced lateral surface migration of Ga atoms along <1-100> directions [10, 21].

Figs. 3(a) and [(b)-(d)] show the RT-PL and LT-PL spectra of (11-22) GaN on m-planar and HP-SiO₂, respectively. As shown in Fig. 3(a), the integrated RT-PL intensity of (11-22) GaN on HP-SiO₂ was increased by approximately 3 times than on m-planar, which is due to the improvement in crystal quality and extraction efficiency. In the Figs. 3(b)-(d), the LT-PL spectra at 3.32 eV, 3.42 eV and 3.48 eV are related with the partial dislocations (PDs), basal stacking fault (BSFs) and near-band-edge (NBE) emission, respectively [22-24]. As shown in Table 1, the ratio of the integrated intensity of the BSFs to the NBE (I_{BSFs}/I_{NBE}) decreased from 81 to 38 for (11-22) GaN on m-planar and on HP-SiO₂, respectively. The ratio of the intensity of the PDs to the NBE (I_{PDs}/I_{NBE}) also decreased from 38 to 14. These results indicated that the BSFs and PDs of (11-22) GaN layers were effectively decreased by introducing HP-SiO₂.

Figs 4(a)-(b) show the FWHMs of x-ray rocking curves of on-axis and off-axis planes of GaN layers.

The FWHMs of the on-axis (11-22) XRC at $\phi = 0^\circ$ and 90° were reported to be associated with partial dislocations (PDs) with PDs and/or prismatic stacking faults (PSFs), respectively [25]. As shown in Fig. 4(a), the FWHMs of GaN on HP-SiO₂ were narrower by approximately 70% at c-axis, and 210% at m-axis, than those of m-planar, respectively, which indicates the crystal quality improvement of (11-22) semipolar GaN layers on HP-SiO₂. The FWHMs of off-axis planes such as (10-10), (11-20), and (0002) are shown in Fig. 4(b) with an inclination angle χ with respect to (11-22) at various azimuths. The off-axis plane peaks of (10-10) and (0002) were broadened by basal stacking faults (BSFs) and PDs and/or perfect dislocations, respectively [25]. According to the results, the FWHMs of GaN on HP-SiO₂ were decreased by approximately 13% in (10-10) and 240% in (0002), compared with those of GaN on m-planar, respectively, which indicates that semipolar

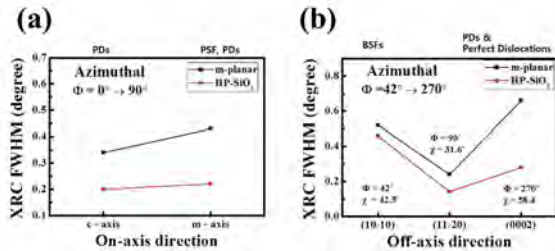


Fig. 4. DC-XRD results showing FWHMs of (a) on-axis and (b) off-axis planes of GaN layers.

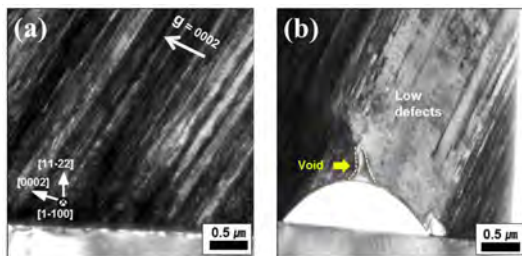


Fig. 5. Cross-sectional TEM images of the GaN layers on (a) m-planar, (b) HP-SiO₂. (BF $z = [1-100]$, $g = 0002$).

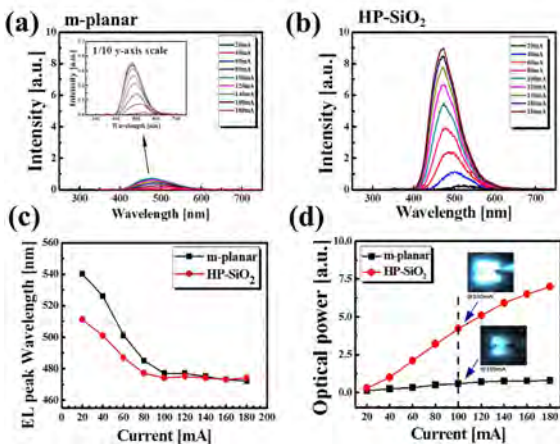


Fig. 6. Electroluminescence results of semipolar InGaN QW LEDs. (a)-(c) Peak wavelength change and (d) Optical power change as a function of injection current. (Insets of (d) show the EL images).

GaN layers grown on HP-SiO₂ have much lower defects such as both BSFs and partial/perfect dislocations. Especially, it is obvious the reduction of FWHM of (0002) broadened by PDs and/or perfect dislocations.

Figs.5(a)-(b) show the cross-sectional TEM images of semipolar GaN layers on m-planar and HP-SiO₂ substrates, respectively. The electron diffraction is taken along $z = [1-100]$ with $g = (0002)$, and it should be noted that only partial dislocations and several types of dislocations are observable in this orientation [22, 26]. As shown in the TEM images, a large number of dislocations were generated in (11-22) GaN grown on m-planar, in comparison with that on of HP-SiO₂. As shown in Fig. 5(b), low defect area as shown in (11-22) GaN on HP-SiO₂ compared with that of m-planar, which indicates that the HP-SiO₂ mask had a considerable effect on the reduction of partial and perfect dislocations. The cross-sectional TEM observation supports the reduction of FWHMs of the (0002) off-axis plane of GaN on HP-SiO₂ in comparison with m-planar, as shown in Fig. 4(b).

Figures 6[(a)-(c)] and (d) show peak wavelength and optical power as a function of injection current in the EL measurement of the semipolar InGaN/GaN LEDs on m-planar, and HP-SiO₂ substrates. Figs. 6(a)-(c) show the peak wavelength changes of the LEDs on m-planar and HP-SiO₂ are 69 nm and 37 nm, respectively. The wavelength change is attributed to the potential fluctuations by Indium segregation related with defects [27-28]. Therefore, this result indicates that the MQWs of HP-SiO₂ LED were formed with better quality than that of m-planar. In addition, Fig. 6(d), the optical power of the LEDs at 100 mA on HP-SiO₂ substrates increased by 6 times compared with that of m-planar LED.

Conclusions

In conclusion, we proposed ELO technology using a HP-SiO₂ mask when (11-22) semipolar GaN layers were grown on m-sapphire. Semipolar GaN grown on planar m-sapphire has a very high density of defects such as partial/perfect dislocations and BSFs. Semipolar GaN and InGaN/GaN LED growth on HP-SiO₂ showed the better crystal quality and optical properties in comparison with that of m-planar, which suggests that HP-SiO₂ is a promising technique for growing high performance semipolar InGaN LEDs.

Acknowledgment

This work was supported by Industrial Strategic Technology Development Program No. 10041188 of the Ministry of Knowledge Economy and the National Research Foundation of Korea (NRF) grant funded by the South Korean government (MEST) No.2012R1A2A2A01011702.

References

1. S.J. Chang, W.C. Lai, Y.K. Su, J.F. Chen, C.H. Liu, and U.H. Liaw, *IEEE J. on Selected Topics in Quantum Electronics*. 8 (2002) 2.
2. T. Mukai, M. Yamada and S. Nakamura, *Jpn. J. Appl. Phys.* 38 (1999) 3976-3981.
3. O. Ambacher, R. Dimitrov, M. Stutzmann, B.E. Foutz, M.J. Murphy, J.A. Smart, J.R. Shealy, N.G. Weiman, K. Chu, M. Chumbes, B. Green, A.J. Sierakowski, W.J. Schaff, and L.F. Eastman, *Phys. Stat. Sol. (b)* 216 (1999) 381.
4. M.B. Nardelli, K. Rapcewicz, and J. Bernholc, *Appl. Phys. Lett.* 71 (1997) 21.
5. P. Waltereit, O. Brandt, A. Trampert, H.T. Grahn, J. Menniger, M. Ramsteiner, M. Reiche & K.H. Ploog, *Nature*. 406 (2000) 24.
6. A.E. Romanov, T.J. Baker, S. Nakamura, and J.S. Speck, *J. Appl. Phys.* 100 (2006) 023-522.
7. S.M. Hwang, Y.G. Seo, K.H. Baik, I.S. Cho, J. H. Baek, S.K. Jung, T.G. Kim, and M.W. Cho, *Appl. Phys. Lett.* 95 (2009) 071-101.
8. K. Iso, H. Yamada, H. Hirasawa, N. Fellows, M. Saito, K. Fujito, S. P. Denbaars, J.S. Speck, and S. Nakamura, *Jpn. J. Appl. Phys.* 46 (2007) L960-L962.
9. R. Sharma, P.M. Pattison, and H. Masui, *Appl. Phys. Lett.* 87 (2005) 231-110.
10. D.S. Oh, J.J. Jang, O.H. Nam, K.M. Song, S.N. Lee, *J. Cryst. Growth*. 326 (2011) 33-36.
11. A. Strittmatter, J.E. Northrup, N.M. Johnson, M.V. Kisin, P. Spiberg, H. El-Ghoroury, A. Usikov, and A. Syrkin, *Phys. Status Solidi B*. 248 (2011) 561-573.
12. T. Guhne, Z. Bougrioua, P. Vennegues, M. Leroux, and M. Albrecht, *J. Appl. Phys.* 101 (2007) 113101.
13. K. Xing, Y. Gong, J. Bai, and T. Wang: *Appl. Phys. Lett.* 99 (2011) 181-907.
14. X. Ni, . zgtr, A. A. Baski, and H. Morko: *Appl. Phys. Lett.* 90 (2007) 182109.
15. T. Wunderer et al., *Phys. Stat. Sol.* 7 (2009).
16. N. Kriouche et al., *J. Cryst. Growth*. 312 (2010) 2625-2630.
17. J.J. Jang, K.H. Lee, J.H. Hwang, J.C. Jung, S.A. Lee, K.H. Lee, B.H. Kong, H.G. Cho, O.H. Nam, *J. Cryst. Growth*. 362 (2012) 166-170.
18. D.H. Jang, J.I. Shim and K.Y. Yoo, *J. Korean Phys. Soc.* 54 (2009) 2373-2377.
19. T. Tanikawa, T. Hikosaka, Y. Honda, M. Yamaguchi, and N. Sawaki, *Phys. Stat. Sol. (c)* 5 (2008) 2966-2968.
20. S.N. Lee, K.K. Kim, O.H. Nam, J.H. Kim and H. Kim, *Phys. Stat. Sol. (c)* 5 (2010) 2043-2045.
21. K. Hiramatsu, *J. Phys.: Condens. Matter*. 13 (2001) 6961-6975.
22. T. Guhne, Z. Bougrioua, P. Venne, gue, s, M. Leroux, and M. Albrecht, *J. Appl. Phys.* 101 (2007) 113-101.
23. P. de Mierry, N. Kriouche, M. Nemoz, S. Chenot, and G. Nataf, *Appl. Phys. Lett.* Vol. 96 (2010) 231-918.
24. I. Tischer, M. Feneberg, M. Schirra, H. Yacoub, R. Sauer, K. Thonke, T. Wunderer, F. Scholz, L. Dieterle, E. Muller, and D. Gerthsen, *phys. Stat. Sol. B*. 248 [3] (2011) 611-615.
25. Q. Sun, B. Leung, C.D. Yerino, Y. Zhang, and J. Han, *Appl. Phys. Lett.* 95 (2009) 231-904.
26. Y.A.R. Dasilva, M.P. Chauvat, P. Ruterana, L. Lahourcade, E. Monroy and G. Nataf, *J. Phys.: Condens. Matter*. 22 (2010) 355-802.
27. S.A. Lee, J.J. Jang, K.H. Lee, J.H. Hwang, J.C. Jeong, and O.H. Nam, *Phys. Status Solidi A8*. (2012) 1526-1529.
28. H. Sato, A. Tyagi, H. Zhong, R.B. Chung, M. Saito, K. Fujito, J.S. Speck, S.P. DenBaars, and S. Nakamura, *Phys. Stat. Sol. (RRL)* 1 (2007) 162-164.